

## LUMINOUS COMPACT BLUE GALAXIES IN THE LOCAL UNIVERSE

JESSICA K. WERK, ANNA JANGREN, AND JOHN J. SALZER

Astronomy Department, Wesleyan University, Middletown, CT 06459; jessica@astro.wesleyan.edu, anna@astro.wesleyan.edu, slaz@astro.wesleyan.edu

*Submitted 30 June 2004; Accepted 30 August 2004 – To appear in 20 December 2004 ApJ*

### ABSTRACT

We use the KPNO International Spectroscopic Survey (KISS) for emission-line galaxies to identify and describe a sample of local analogues to the luminous compact blue galaxies (LCBGs) that are observed to be abundant at intermediate and high redshift. The sample is selected using criteria believed effective at isolating true examples of LCBGs:  $SB_e(\text{B-band}) < 21.0 \text{ mag arcsec}^{-2}$ ,  $M_B < -18.5$  (for  $H_0 = 75 \text{ km s}^{-1} \text{ Mpc}^{-1}$ ), and  $B - V < 0.6$ . Additionally, all LCBG candidates presented are selected to have star-formation as their dominant form of activity. We examine the properties of our LCBGs and compare them to those of other KISS star-forming galaxies of the same absolute magnitude range. We find that the KISS LCBGs lie on the extreme end of a fairly continuous distribution of “normal” star-forming galaxies in the plane of surface brightness versus color. This result differs from the results of previous studies that show LCBGs at higher- $z$  to be more separate from the “normal” (usually non-active) galaxies they are compared against. On average, LCBGs have a higher tendency to emit detectable flux in the radio continuum, have higher H $\alpha$  luminosities by a factor of 1.6, indicating strong star-formation activity, and have slightly lower than expected metal abundances based on the luminosity-metallicity relation for KISS galaxies. We calculate the volume density of our low- $z$  ( $z < 0.045$ ) sample to be  $5.4 \times 10^{-4} h_{75}^3 \text{ Mpc}^{-3}$ , approximately 4 times lower than the volume density of the LCBGs at  $0.4 < z < 0.7$  and  $\sim 10$  times lower than the volume density of the population at  $0.7 < z < 1.0$ .

*Subject headings:* galaxies: starburst — galaxies: active — galaxies: evolution — galaxies: structure

### 1. INTRODUCTION

Common at intermediate and high redshifts, yet rare in the local universe, luminous compact blue galaxies (LCBGs) typically have luminosities equal to or greater than that of the Milky Way but are considerably smaller in size (Koo *et al.* 1994; Phillips *et al.* 1997; Guzmán *et al.* 1997; Östlin *et al.* 2001; Mallén-Ornelas *et al.* 1999). As evidenced by such properties, they are among the most extreme galaxies known in the universe. Although these galaxies have been the subject of numerous comprehensive studies in the past decade, their evolution and nature, to a large extent, remains in dispute (Koo *et al.* 1995; Phillips *et al.* 1997; Hammer *et al.* 2001; Östlin *et al.* 2001; Barton & van Zee 2001; Pisano *et al.* 2001; Guzmán *et al.* 2003). At the heart of the issue lies the difficulty of identifying nearby analogues that would allow a more complete exploration of the mechanisms responsible for their extreme properties at high redshifts, as well as their evolutionary paths.

Characterized by high surface brightnesses, small half-light radii, and vigorous star-formation, LCBGs were initially identified as stellar objects from 4-m plate surveys for QSO candidates (Koo & Kron 1992; Koo *et al.* 1994; Guzmán *et al.* 1996, 1998). The formal definition of LCBGs is developed by Jangren *et al.* (2004) from examining regions of six-dimensional parameter space (color, luminosity, asymmetry, concentration, size, and surface brightness) occupied by three classes of compact galaxies chosen to represent the population of luminous, blue, compact galaxies as a whole. The three classes are: (1) Compact Narrow Emission-Line Galaxies (CNELGs, Koo *et al.* 1994, 1995; Guzmán 1996,

1998), (2) a subset of galaxies very similar to CNELGs studied by Koo *et al.* (1995); Phillips *et al.* (1997) and Guzmán *et al.* (1997) called faint blue galaxies, and (3) higher redshift Blue Nucleated Galaxies (BNGs, Schade *et al.* 1995, 1996). While the classification of an LCBG relies on the galaxy’s falling within three of five defined regions in the aforementioned parameter space, recently groups have adopted three cut-offs that roughly correspond to the criteria laid out by Jangren *et al.* (2004):  $B - V < 0.5 - 0.6$ ,  $SB_e < 21 - 21.5 \text{ mag arcsec}^{-2}$ , and  $M_B < -18.5$ , with  $H_0 = 70 \text{ km s}^{-1} \text{ Mpc}^{-1}$  (Garland *et al.* 2004; Pisano *et al.* 2001). These selection criteria will be further examined in subsequent sections.

With a volume density that drops off substantially from  $z = 1$  to the present (previously estimated to be a change of roughly a factor of ten), LCBGs appear to be the most strongly evolving galaxy population (Lilly *et al.* 1996; Phillips *et al.* 1997; Guzmán *et al.* 1997; Lilly *et al.* 1998; Mallén-Ornelas *et al.* 1999). Guzmán *et al.* (1997) estimate that they contribute nearly 40% of the fractional increase in the SFR density between  $z = 0$  and  $z = 1$ . Furthermore, luminous, compact star-forming galaxies appear to dominate high-redshift galaxy samples. Lowenthal *et al.* (1997) have suggested that the Lyman Break Galaxies at  $z = 3$ , due to their very compact cores and high surface brightnesses, may be the high-redshift counterparts of the intermediate- $z$  LCBGs. Smail *et al.* (1998), in a sub-millimeter galaxy survey, found a  $z \sim 4$  galaxy population that may contribute a substantial fraction of the SFR density in the early universe, nearly half of which are very luminous and compact. Evidently, LCBGs play

a prominent, if not paramount, role in the formation and evolution of galaxies in the young universe.

A drove of unanswered questions hovers around the subject of LCBGs, mainly owing to the lack of a representative local sample. One of these questions involves the mechanism(s) responsible for the observed intense starbursts in LCBGs. In theory, these triggering mechanisms could be determined by examining the  $H\alpha$  velocity fields and morphologies of local LCBG examples (Östlin *et al.* 2001). This sort of study relies on the assumption that one can select a sample of local LCBGs to have the same properties as the more distant LCBGs. Östlin *et al.* (2001) use a sample of six galaxies with  $M_B$  between -17.5 and -20 selected from local blue compact galaxies (BCGs) that are bright in  $H\alpha$  to infer certain kinematic properties of the higher- $z$  LCBGs. They conclude that, in most cases, mergers or strong interactions trigger the intense starbursts of LCBGs. However, one should use caution in interpreting these results given the size and properties of their sample. Indeed, a statistically complete sample of low- $z$  LCBGs will provide more clues as to the the origin of their activity.

Another crucial topic in the study of LCBGs has been the question of what sort(s) of galaxy they become as they evolve. The determination of reliable mass estimates for the intermediate- $z$  LCBGs is key to establishing these evolutionary connections to present-day galaxies. However, accurate stellar mass estimates are difficult to determine and measurements of emission-line widths used to indicate the virial mass may underrepresent the gravitational potential for the intermediate-redshift LCBGs (Guzmán 2001; Guzmán *et al.* 2003; Pisano *et al.* 2001). As a consequence of these difficulties, there is not good agreement for the mass estimates of LCBGs and there is a corresponding uncertainty as to their proposed evolutionary path(s). Phillips *et al.* (1997), Barton & van Zee (2001), and Hammer *et al.* (2001) argue for an evolutionary scenario in which LCBGs represent the formation of the bulges of objects that will eventually evolve into massive spiral disks of today. Koo *et al.* (1995), and Guzmán *et al.* (1996, 1997, 1998) maintain that while LCBGs represent a heterogeneous class of galaxies, the majority will evolve into local low-mass dwarf elliptical galaxies.

A possible solution to the mass debate may lie in the HI line widths of local LCBGs. These line widths can be used to infer the total dynamical mass. Accordingly, Pisano *et al.* (2001) set out to measure the HI line widths of a nearby sample of galaxies they believe are representative of the more distant LCBGs. They infer the masses of the intermediate- $z$  galaxies from these local examples, and find that LCBGs have a variety of dynamical masses, and thus a variety of evolutionary paths. Yet, they recognize that their local sample may not have been truly representative of the the high- $z$  LCBG population. Of their 11 local galaxies, only three meet the criteria proposed by Jangren *et al.* (2004). In a study of 20 local LCBG candidates selected to more nearly meet the the criteria of Jangren *et al.* (2004), Garland *et al.* (2004) found results similar to those of Pisano *et al.* (2001). Specifically, they show that while most LCBGs are nearly ten times less massive than local galaxies of the same luminosity, some are just as massive. The implication is that

LCBGs are a heterogeneous class of galaxy.

Clearly, defining reliable local samples of LCBGs is central to the process of understanding their nature and evolutionary paths. The Pisano *et al.* (2001) and Garland *et al.* (2004) samples are recent attempts to construct samples of nearby LCBGs. The latter study is based on a sample of LCBGs discovered by Castander *et al.* (2004) who analyzed data from the Sloan Digital Sky Survey. Another recent study by Drinkwater *et al.* (1999) utilized the complete spectroscopic study of a 12 deg<sup>2</sup> area centered on the Fornax Cluster to identify a sample of 13 LCBGs with redshifts less than 0.21. In the current study, we take a slightly different approach.

Using the KPNO International Spectroscopic Survey (KISS, Salzer *et al.* 2000), we aim to identify and describe a statistically complete local sample of star-forming galaxies that best resemble those LCBGs observed in the more distant universe. Our low- $z$  sample will provide a basis for future work aimed at resolving the debates over the evolutionary histories and kinematics of LCBGs. Due to the limited resolution of the survey images, the classification scheme developed by Jangren *et al.* (2004), that uses morphological parameters, cannot be employed. Instead, we apply selection criteria consistent with the parameters of Jangren *et al.* (2004) as a way to isolate the LCBGs from other KISS star-forming galaxies. While sharp boundaries in parameter space do not always effectively isolate one type of galaxy from another, LCBGs in the color-surface brightness plane occupy a well-defined region of parameter-space (Jangren *et al.* 2004). Therefore, we employ criteria in  $B-V$  color, in surface-brightness, and in luminosity to select a sample of local LCBG candidates. Still, none of the selection criteria we use can guarantee that the KISS LCBG candidates, like other putative local samples, will contain *bona fide* LCBGs; they only insure a similarity. Regardless, we believe that the sample we define will provide an adequate starting point for future investigation. In § 2, we describe KISS, our measurements, and selection criteria. An analysis of the properties of our local LCBGs along with the volume density calculation appears in § 3. Section 4 contains a discussion of the implications our sample has for high- $z$  studies and potential future work on these galaxies beyond KISS. In § 5, we summarize our results. Throughout this paper we adopt  $H_0 = 75$  km s<sup>-1</sup> Mpc<sup>-1</sup>.

## 2. THE DATA

### 2.1. KPNO International Spectroscopic Survey

The KPNO International Spectroscopic Survey (KISS) aims to find a quantifiably complete, well-defined sample of extragalactic emission-line sources (Salzer *et al.* 2000). Although this survey is not the first to look for galaxies that display unusual activity, it reaches substantially deeper than other wide-field objective-prism surveys, mainly because it *is* the first survey of this type to employ a large-format CCD as its detector. The survey data, composed of both objective-prism and direct images, were taken with the 0.61 m Burrell Schmidt telescope located on Kitt Peak. The objective-prism images cover a spectral range of either 4800 - 5500 Å or 6400 - 7200 Å and the direct images are observed through standard  $B$  and  $V$  filters. Our local sample of LCBGs is

derived from the first three KISS survey strips: KISS red list 1 (KR1), described in Salzer *et al.* (2001); KISS blue list 1 (KB1), described in Salzer *et al.* (2001b); and KISS red list 2 (KR2), described in Gronwall *et al.* (2004c). KR1 and KR2 use the H $\alpha$  line for selection whereas KB1 detects objects by their [OIII] emission line. The KR1 portion of KISS finds 1128 ELG candidates in a survey area of 62.2 deg<sup>2</sup> (or 18.1 KISS ELGs per square degree); the KB1 portion of KISS finds 223 ELG candidates in 116.6 deg<sup>2</sup> (or 1.91 KISS ELGs per square degree); and the KR2 portion of KISS finds 1029 ELG candidates in 65.8 deg<sup>2</sup> (or 15.6 KISS ELGs per square degree). KR1 and KB1 overlap with part of the Century Survey (Geller *et al.* 1997; Wegner *et al.* 2001) while KR2 runs through the center of the Boötes void.

The KISS data are run through several steps of processing using a series of Image Reduction and Analysis Facility<sup>1</sup>(IRAF) scripts: object detection and inventory, photometry and object classification, astrometry, spectral image coordinate mapping and background subtraction, spectral extraction and overlap correction, emission line detection, and spectral parameter measurement. Measurements of the extracted objective-prism spectra yield estimates of the redshifts, line fluxes, and equivalent widths of the ELGs. For a complete description of the data processing, see Salzer *et al.* (2000). It should be noted that many objects are unresolved in the direct images (which have a resolution of  $\sim 4''$ ); it is not necessary for an object to be classified morphologically as a galaxy for inclusion in the ELG list. The only criterion for inclusion is the presence of an emission line in the objective-prism spectrum. In other words, there is no bias against compact, stellar appearing objects in KISS.

Although the survey data themselves provide considerable information about the sources, obtaining follow-up spectra is an important part of the KISS project. These spectra provide higher quality redshifts, confirm ELG candidates' status as actual ELGs, and provide the means by which to identify the type of activity powering the ELG. In most cases, emission lines such as H $\alpha$ , H $\beta$ , [O III]  $\lambda\lambda 4959, 5007$ , and [N II]  $\lambda\lambda 6548, 6583$  are present in the follow-up spectra. With the higher-accuracy line strengths of these spectra, one can distinguish between star-forming galaxies, Seyfert 1 galaxies, Seyfert 2 galaxies, LINERs, and QSOs. Furthermore, determination of the metallicity (Melbourne & Salzer 2002; Melbourne *et al.* 2004; Lee, Salzer & Melbourne 2004; Salzer *et al.* 2004) and the star-formation rate is possible with accurate line-strength measurements. Follow-up spectra have been obtained for 83% of the KR1 ELGs, 100% of the KB1 ELGs, and 30% of the newer KR2 ELGs at various telescopes including the Hobby-Eberly telescope (Gronwall *et al.* 2004a), the Michigan-Dartmouth-MIT 2.4m telescope (Wegner *et al.* 2003), the Wisconsin-Indiana-Yale-NOAO 3.5m, the 2.1m on Kitt Peak, the Apache Point Observatory 3.5m, and the Shane 3.0m telescope at Lick Observatory (Melbourne *et al.* 2004).

<sup>1</sup> IRAF is distributed by the National Optical Astronomy Observatory, which is operated by the Association of Universities for Research in Astronomy, Inc., (AURA) under cooperative agreement with the National Science Foundation.

## 2.2. Surface Brightness and Half-Light Radius Measurements

LCBGs typically are identified by their small half-light radii ( $r_{hl}$ ) and/or their high surface brightnesses ( $SB_e$ ). Therefore, measuring these quantities in the KISS data was an essential first step in our effort to isolate a sample of nearby LCBGs. We wrote an IRAF procedure called KCOMPACT to find  $r_{hl}$  for every object in the KISS survey images. The procedure performs a curve of growth analysis using circular apertures to determine  $r_{hl}$ . The formal uncertainty in  $r_{hl}$  is estimated by comparing the separate measurements of ELGs present in two survey fields (the overlap in adjacent KISS fields is approximately 3-5 arcminutes). Based on 14 objects, we determine the uncertainty in  $r_{hl}$  to be 0.21 arcseconds. Combining our estimates of  $r_{hl}$  with the total apparent magnitude measured during the KISS data processing (see § 2.1) allows us to compute  $SB_e$  using the following formula:

$$SB_e = m_B + 0.753 + 2.5 \log \pi r_{hl}^2 \quad (1)$$

As the formal errors in the KISS apparent magnitudes are always below 0.1 magnitude, we can find the upper limit on the uncertainty of  $SB_e$  due to the errors in  $m_B$  and  $r_{hl}$ . We find  $\sigma_{SB_e} < 0.14$  mag arcsec<sup>-2</sup>.

The reliability of  $r_{hl}$  and  $SB_e$  is inextricably linked to the resolution of the image on which they are measured. Both the image scale and the effective seeing significantly affect the accuracy of these quantities. Resolution limits restrict the precision with which these quantities can be determined in the more distant portion of KISS. Since *all* objects in each survey image are analyzed by KCOMPACT, we use the locus of the  $r_{hl}$  values for objects previously identified as stars to define a rough resolution limit for each image. Marked interactively, the resolution limit represents not the mean FWHM of the stellar distribution but rather is selected to encompass the entire locus of stellar objects. As we will discuss in the following paragraph, variable image quality across our survey images causes this limit to underestimate the true image quality for a modest fraction of our ELG candidates. For KB1 and KR1, the mean resolution limit (i.e., the lower limit on  $r_{hl}$ ) of the images is 2.50" compared to an image scale of 2.03"/pixel; for KR2, this mean resolution limit of the images is 2.13" compared to an image scale of 1.43"/pixel. Therefore, objects with  $r_{hl}$  under 2.5" are almost always unresolved (or, at best, marginally resolved) in the KISS survey direct images. Moreover, as the distance to an object increases, so does the physical diameter that corresponds to this resolution limit. That is to say, at greater distances, galaxies with progressively larger diameters dominate any resolved sample. Figure 1 shows this effect, plotting diameter in kpc vs. distance in Mpc, where the diagonal lines represent the nearly constant resolution limits (converted to kiloparsecs) below which an object is unresolved. Everything but galaxies with large diameters will be unresolved at the redshift limit of the survey. Ultimately, this bias leads us to adopt a distance-limited sample of KISS LCBGs (see section 2.3).

The rough resolution limit discussed in the previous paragraph suffices for a determination of an appropriate distance-cut (see below), but fails to account for the rather extreme image quality variability of the KISS di-

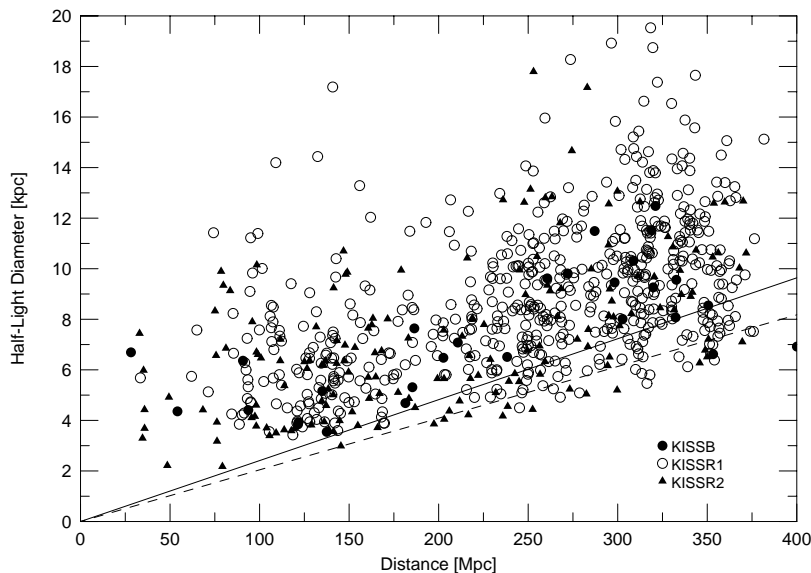


FIG. 1.— The half-light diameter in kpc versus the distance in Mpc for a subset of KISS star-forming galaxies from each survey strip. The dashed diagonal line represents the diameter (in kpc) necessary for a KR2 object to be resolved at a given distance (based on the rough resolution limit discussed in section 2.2). The solid diagonal line represents the diameter (in kpc) necessary for KB1 and KR1 objects to be resolved at a given distance. Below these diagonal lines, galaxies from their respective survey lists are unresolved.

rect images. The delivered image quality of the Burrell-Schmidt 0.61-m at the time KISS was carried out could vary between  $2.5''$  and  $6.5''$  over a single survey field. Hence, rather than use a single value to describe the image quality on a given survey image, it is necessary to estimate the local value for the image quality in the vicinity of each KISS ELG. An IRAF script was written for this purpose. By locating the ten closest stars to each ELG and measuring the FWHM of their profiles, this script accounts for the variable image quality of the KISS direct images. The local FWHM (average seeing) for each KISS ELG is the mean of the FWHM from the ten stellar profiles. As our study relies upon accurate measurements of  $r_{hl}$  and  $SB_e$ , we were forced to exclude those objects for which the local image quality was severely degraded. A ratio between the mean local FWHM and the half-light diameter acted as our main diagnostic: if the ratio were above 1, we could not trust the measurement of  $r_{hl}$ , and therefore we exclude the galaxy. In addition, all objects with the local stellar FWHM above  $5''$  and a diagnostic ratio above 0.7 were also excluded. In total 96 galaxies were cut out of the survey area, decreasing the area over which we could search for LCBGs by only  $\sim 4\%$ . With these exclusions, we feel confident in the completeness of our sample. That is, in the remaining portions of KISS we should not miss any apparently small, potential LCBG candidate simply because it is under-resolved. Of course, the galaxies remaining in our sample of KISS ELGs are not all well-resolved, but as we will describe, we can account for the inaccuracies in their measurements.

In essence, our measurements of marginally resolved galaxies act as upper limits on  $r_{hl}$  and lower limits on  $SB_e$ . We explore the nature of our unresolved and marginally resolved LCBG candidates us-

ing higher-resolution images from the Wisconsin Indiana Yale NOAO (WIYN) 0.9 m telescope on Kitt Peak. In May 2003 and March 2004 we observed 11 KISS ELGs from KR1 and 12 KISS ELGs from KR2 under non-photometric conditions with the S2KB CCD, for which the image scale is 0.6 arcsec/pixel. The pre-existing KISS direct images for the galaxies, that were taken under good conditions, provided the photometric calibration for our 0.9-m images. Despite the different image scales of KR1 and KR2, we treat them the same in the following analysis due to the variable image quality described above.

For the KISS compact, star-forming ELGs in each survey strip, we re-measured the half-light radii on the 0.9-m images using the same curve-of-growth routine described above, and compared them with the values of  $r_{hl}$  obtained in the same way for the KISS images. The KISS  $r_{hl}$  is plotted against the ratio of the 0.9-m  $r_{hl}$  to the KISS  $r_{hl}$  in Figure 2a to show the results of these re-measurements. The triangles represent the ELGs from KR2, while the circles represent the ELGs from KR1. The relationship is equivalent for both strips: those objects with larger  $r_{hl}$  have a ratio close to unity, while those objects with  $r_{hl}$  near our resolution limits have ratios that deviate more considerably from unity.

We sought to quantify the correlation seen in Figure 2a in order to develop a correction of  $r_{hl}$  for all unresolved and marginally resolved ELGs in the KISS database. Analyzing our sets of measurements for the 0.9-m images and the KISS images, we can predict the way in that the difference between a galaxy's 0.9-m  $r_{hl}$  and its KISS  $r_{hl}$  ( $\Delta r_{hl}$ ) increases as its  $r_{hl}$  decreases below the resolution limits of KISS. Instead of re-observing all unresolved and marginally resolved KISS ELGs to achieve

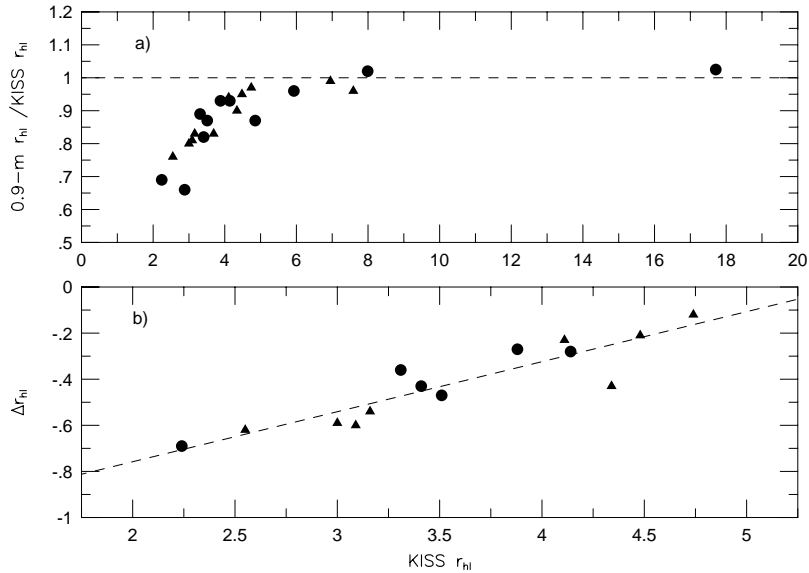


FIG. 2.— a) A plot of the ratio of the  $r_{hl}$  re-measured on the 0.9-m images (0.9-m  $r_{hl}$ ) to the  $r_{hl}$  measured on the KISS direct images (KISS  $r_{hl}$ ) versus the KISS  $r_{hl}$ . The filled circles represent ELGs from KR1, and the filled triangles represent ELGs from KR2. At an  $r_{hl}$  of approximately 5 arcseconds, the ratio of the two quantities is very close to one. b) This plot shows the observed relation between  $\Delta r_{hl}$  (0.9-m  $r_{hl}$  - KISS  $r_{hl}$ ) and the KISS  $r_{hl}$ . Plot symbols are the same as in a). The linear-least-squares fit shown by the dashed line was used to apply a correction for the  $r_{hl}$  of all KISS star-forming ELGs with  $r_{hl}$  below 5 arcseconds.

more accurate measurements of their  $r_{hl}$ , we can infer the values we would obtain. Two of the eleven KR1 and two of the twelve KR2 ELGs observed with the WIYN telescope had  $r_{hl}$  greater than 6.0 arcseconds, and were thus very well-resolved in the KISS direct images. Figure 2a reassures us that our measurements of  $r_{hl}$  on the 0.9-m images are very close to our measurements on the KISS images for these four well-resolved galaxies. These four galaxies were excluded from the determination of our correction. Upon closer examination of the 0.9-m images, one galaxy in KR1 was observed to have a merging partner, making suspect any measurement of its  $r_{hl}$ . An additional two galaxies from each survey strip were excluded as well because they suffered from noticeably poorer image quality in the KISS direct images, skewing the relationships shown in the following plots. Figure 2b shows  $\Delta r_{hl}$  versus the KISS  $r_{hl}$  for the 14 remaining galaxies. In this figure, we notice the same effect as in Figure 2a: apparently smaller galaxies have greater  $\Delta r_{hl}$ . We based the final correction for  $r_{hl}$  upon the linear-least squares fit of the 14 data points plotted in Figure 2b. The fit is shown by the dashed line. The equation for this line is:  $\Delta r_{hl} = 0.22(\text{KISS } r_{hl}) - 1.19$ , where  $\Delta r_{hl}$  is in arcseconds, and the scatter about the fit is 0.11 arcseconds.

We also compared the apparent B-band magnitudes ( $m_B$ ) measured on the 0.9-m and KISS images. Since our photometric calibration of the 0.9-m images made use of the original KISS calibration, our 0.9-m values for  $m_B$  agree well with the KISS values for  $m_B$ . This re-measurement of  $m_B$  combined with the correction for  $r_{hl}$ , described above, is relevant for probing the effects of low-resolution upon the measurement of  $SB_e$  (see equation

1). Figure 3 plots the observed relation between  $\Delta SB_e$  (0.9-m  $SB_e$  - KISS  $SB_e$ ) and  $\Delta r_{hl}$ . Since the KISS and 0.9-m apparent magnitudes show good agreement, the difference in the measured values of  $SB_e$  must be due to solely the change in  $r_{hl}$  between the KISS and 0.9-m images. Therefore we can compute the correction for the effective surface brightness,  $\Delta SB_e$ , such that it depends on only  $\Delta r_{hl}$ .

$$\Delta SB_e = -2.5 \log \frac{r_{hl}^2}{(r_{hl} + \Delta r_{hl})^2} \quad (2)$$

Figure 3 plots the observed values of  $\Delta SB_e$  and  $\Delta r_{hl}$  for the 14 KISS ELGs along with a curve illustrating the analytical correction given by equation 2. The observed values of  $\Delta r_{hl}$  and  $\Delta SB_e$  are shown by the filled triangles (KR2) and the filled circles (KR1). In the equation,  $\Delta r_{hl}$  corresponds to the linear-least-squares fit shown in Figure 2b for the  $r_{hl}$  correction. Figure 3 shows that the actual measurements of  $\Delta r_{hl}$  and  $\Delta SB_e$  follow the correction defined by equation 2 very well.

We apply these corrections for  $r_{hl}$  and  $SB_e$  to all non-excluded (see above) KISS star-forming galaxies with an  $r_{hl}$  less than 5 arcseconds. Among all KR1 star-forming ELGs with  $r_{hl}$  under 5 arcseconds (i.e., those affected by the correction), the mean change in  $r_{hl}$  is -0.50 arcseconds, the mean change in diameter is -4.91 kpc, and the mean change in  $SB_e$  is -0.44 mag arcsec<sup>-2</sup>. Among all KR2 star-forming ELGs with  $r_{hl}$  under 5 arcseconds, the mean change in  $r_{hl}$  is -0.56 arcseconds, the mean change in diameter is -5.31 kpc, and the mean change in  $SB_e$  is -0.57 mag arcsec<sup>-2</sup>.

### 2.3. Sample Selection

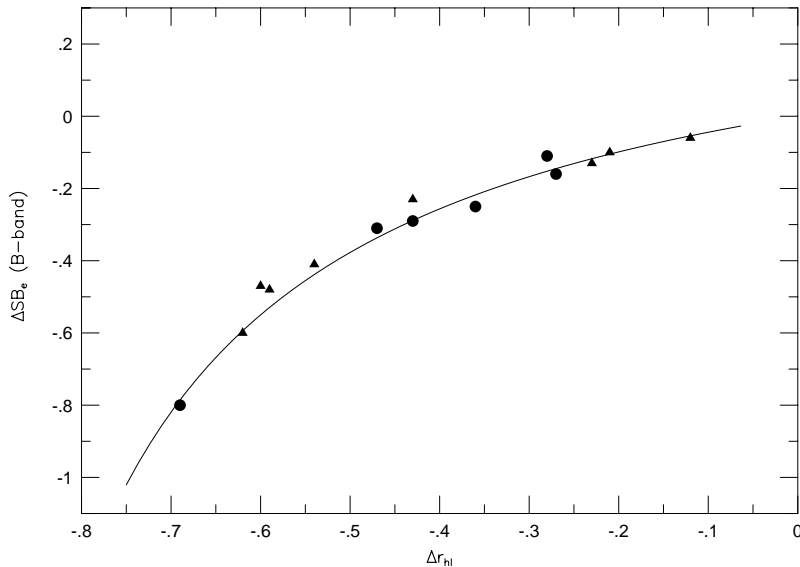


FIG. 3.— The observed relation between  $\Delta SB_e$  ( $0.9\text{-m } SB_e - \text{KISS } SB_e$ ) and  $\Delta r_{hl}$  shown by the filled circles and triangles plotted with the analytical correction curve given by the equation  $\Delta SB_e = -2.5 \log \frac{r_{hl}^2}{(r_{hl} + \Delta r_{hl})^2}$ . The circles represent KR1 galaxies, while the triangles represent KR2 galaxies.  $\Delta r_{hl}$  is based upon the correction for  $r_{hl}$ , given by the linear-least-squares fit shown in Figure 2.

The ability of our local LCBG candidates to provide meaningful mass and SFR comparisons with the higher- $z$  LCBGs requires that these galaxies be genuine LCBGs. Typical methods of identifying nearby LCBG analogues usually employ cut-offs in surface brightness, luminosity, and color, and cannot guarantee that the galaxies are true examples of LCBGs. Indeed, we only can pick out those galaxies that are *likely* to be LCBGs. Considering the nature of KISS, we believe that we are identifying those ELGs that possess the same properties as the LCBGs at intermediate and high redshifts, and thus, those galaxies that are most likely to be true LCBGs. Hence, we call our galaxies LCBG candidates.

In an attempt to match our KISS LCBG sample with the higher-redshift samples, we endeavor to employ the same cut-offs as those used in earlier work. The sample is based on criteria proposed by Guzmán (2003), who uses cut-offs in surface brightness, rest-frame color, and absolute magnitude for the selection of LCBGs. All criteria are limited by the angular resolution of the KISS survey direct images. Certainly, LCBGs are *not* AGN, and are most often characterized by vigorous star-formation. Therefore the sample was selected from a subsample of KISS galaxies known from follow-up spectra to have star-formation as their primary form of activity. All values given for  $B-V$  color and all magnitudes used in the KISS sample selection are corrected for Galactic absorption using the values of Schlegel, Finkbeiner, & Davis (1998). Additionally, to select this sample, we used the corrected values of  $SB_e$  determined from the analysis outlined in the previous section.

A total of 17 KISS star-forming galaxies meet the selection criteria proposed by R. Guzmán:  $SB_e$  ( $B$ -Band)  $< 21.0 \text{ mag arcsec}^{-2}$ ,  $M_B < -18.5$ ,  $B - V < 0.6$  with

$H_0 = 70 \text{ km s}^{-1} \text{ Mpc}^{-1}$ . We use this absolute magnitude limit for the selection of KISS LCBGs despite our use of  $H_0 = 75 \text{ km s}^{-1} \text{ Mpc}^{-1}$  by KISS. Since this absolute magnitude cut corresponds to  $M_B < -18.35$  with  $H_0 = 75 \text{ km s}^{-1} \text{ Mpc}^{-1}$ , we apply a slightly more stringent cut for absolute magnitude by 0.15 magnitudes when we use  $M_B < -18.5$  as one of our selection criteria.

This sample of LCBGs is partially determined by the resolution selection effects described in Section 2.2 and shown in Figure 1. These effects dictate that the majority of identified LCBG candidates will be located at distances far closer than the KISS redshift limit of  $z = 0.095$ . Considering that the median half-light diameter of the 17 LCBGs is 4.21 kpc, Figure 1 indicates that likelihood of finding an LCBG beyond  $\sim 200 \text{ Mpc}$  is low. A further implication of this effect is that any comparison of the KISS LCBG sample with other KISS star-forming galaxies will be skewed. KISS star-forming galaxies detected at greater distances will be, on average, considerably larger in diameter and more luminous. To account for these effects, and to improve the completeness of our LCBG sample, we impose on it a distance limit of 185 Mpc ( $z \sim 0.045$ ). 16 of the 17 KISS LCBGs lie within this boundary, and according to the resolution thresholds marked on Figure 1, any galaxy within 185 Mpc of the Milky Way with a diameter equal to or greater than  $\sim 4 \text{ kpc}$  will be resolved in the KISS images.

Figure 4 shows KISS ELGs that lie within 185 Mpc of the Milky Way and have  $M_B < -18.5$ . The 16 KISS ELGs that remain in the sample after the application of the distance cut-off are marked as filled circles in the plot, and the dashed lines indicate two of the selection criteria. The stars in the plot represent a subset of “normal” galaxies from the Century Survey

(CS) carried out by Wegner *et al.* (2001) that lie within the distance limit and have  $M_B < -18.5$ . The Century Survey is a traditional magnitude-limited survey of “normal” field galaxies that are used here to represent the general galaxian population. The open circles represent a comparison sample of KISS star-forming ELGs that have  $M_B < -18.5$  and lie within 185 Mpc of the Milky Way. Henceforth, when we refer to our samples of LCBG candidates and comparison samples, we refer to the *distance-limited* samples. It should be noted that all KISS ELGs selected as LCBG candidates have been identified as having star-formation as their primary form of activity from follow-up spectra.

On the plot of  $SB_e$  versus color in Figure 4, two features stand out. While the KISS LCBG candidates were selected to have surface brightnesses higher than the typical star-forming galaxy (SFG), even the highest surface brightness LCBG candidates do not appear to be clearly separated from the distribution of KISS SFGs. Instead, the star-forming galaxies form a more-nearly continuous distribution in color and  $SB_e$ , as one might expect. At intermediate redshifts, Jangren *et al.* (2004) find that in the parameter space of  $SB_e$  and  $B-V$  color, LCBGs separate themselves more cleanly than in any other parameter space from ordinary irregular, elliptical, and spiral galaxies. A plot from Jangren *et al.* (2004) is shown in Figure 5, illustrating this separation. When we compare LCBGs with the other KISS star-forming galaxies, we do not see this effect. In the  $z < 0.045$  local universe, the bluest, highest surface brightness star-forming ELGs do not appear to be separate from a distribution of otherwise regular star-forming galaxies, but rather represent the most extreme galaxies in this class of star-forming ELGs. However, the KISS LCBG candidates are more clearly separate from the CS galaxies. Interesting to note is that while only three of the CS galaxies meet the selection criteria for an LCBG, 29 CS galaxies redder than the color cut meet both the surface brightness and absolute magnitude cut. We believe these 29 galaxies to be local, normal elliptical galaxies. Only 6 KISS ELGs fall in this region of the diagram (i.e., compact but red).

The properties of the 16 ELGs selected as local LCBG candidates are listed in Table 1. Columns 1 and 2 give the survey identification numbers for each galaxy (KISSR and KISSB numbers). The apparent B-band magnitude is listed in column 3, the  $B-V$  color in column 4, the half-light diameter in kiloparsecs in column 5, the B-band effective surface brightness ( $SB_e$ ) in column 6, the distance to the galaxy (in Mpc) in column 7, the absolute B-band magnitude in column 8, the logarithm of the  $H\alpha$  luminosity in column 9, and the logarithm of the 1.4 GHz radio power from Van Duyne *et al.* (2004) in column 10. Those galaxies without a listed radio power were not detected as radio emitters in the Van Duyne *et al.* study.

Images of the 16 LCBG candidates made from the KISS direct images appear in Figure 6. Although the resolution of KISS is too low for measurements of parameters such as asymmetry and concentration, we can see some of the morphological characteristics of our LCBG candidates on these images. At least three of the LCBG candidates, KISSR 147, 1274, and 1870, appear to have disturbed morphologies, evidence for recent interactions and/or mergers. However, the majority of the 16 LCBG

candidates appear to be small, compact, and quite symmetric, suggesting that interactions are not the main driver of the observed star-formation activity in most cases.

### 3. PROPERTIES OF THE LOCAL LCBG CANDIDATES

#### 3.1. Global Characteristics

The KISS project obtains photometrically calibrated B and V direct images along with the objective-prism spectra, that provide accurate measurements of each galaxy’s  $H\alpha$  flux. In addition, all of our LCBG candidates have been observed as part of our follow-up spectroscopy program (e.g., Wegner *et al.* 2003; Gronwall *et al.* 2004a). Hence, there is a large amount of information readily available for all KISS ELGs that allows us to examine the properties of the KISS LCBG candidates in some detail. In this subsection, we present the properties of the LCBG candidates and a comparison sample of KISS star-forming galaxies (SFGs) with  $M_B < -18.5$ . When the necessary data are available, we also present the CS comparison sample of “normal” galaxies that have  $M_B < -18.5$ . All three of these samples are taken from the same volume of space (same area of the sky, and  $D < 185$  Mpc). One implication of this distance limit is that the galaxies in our KISS comparison sample have lower luminosities and bluer colors than the overall sample of star-forming KISS galaxies. In general, the most distant galaxies in any sample tend to be the most luminous, and galaxies that are more luminous tend to be redder.

The B-band absolute magnitudes of the KISS LCBGs, KISS star-forming galaxies, and CS magnitude-limited sample are plotted against  $SB_e$  in Figure 7. Together with Figure 4, these two plots exhibit the selection criteria of the LCBG candidates, and also illustrate nicely the properties of the three galaxy samples. As pointed out in the previous section, the KISS SFG comparison sample exhibits a fairly continuous distribution in all three parameters –  $SB_e$ ,  $M_B$ , and  $B-V$  color – with the LCBG candidates representing the extreme cases in terms of color and surface brightness (Figure 4). The CS and KISS SFG samples overlap substantially in both Figures 4 and 7, although the latter are on average much bluer. The LCBG candidates are seen to be distributed fairly evenly in absolute magnitude between  $-18.6$  to  $-20.6$ . They define the upper envelope of the KISS ELGs in Figure 7.

Figure 8 shows histograms of the half-light diameters of the LCBG candidates, the KISS comparison sample SFGs, and the CS comparison sample “normal” galaxies. The median diameters for the three samples, 4.11 kpc, 6.63 kpc, and 6.43 kpc, respectively, are indicated in the figure. As expected, the KISS LCBGs are, on average, 60% smaller than the CS galaxies and SFGs. The largest LCBGs have sizes comparable to the medians for the other two distributions. Since the samples have comparable luminosities, the difference in diameter accounts for most of the difference in  $SB_e$ .

Figure 9 shows the  $H\alpha$  luminosity plotted against  $M_B$  for the two KISS samples. The sample of 16 KISS LCBG candidates exhibits a higher median  $H\alpha$  luminosity by a factor of 1.6 than the comparison sample SFGs. Because we consider only actively star-forming galaxies in both samples, we can draw an important conclusion from this result. In general, the  $H\alpha$  luminosity indicates the activ-

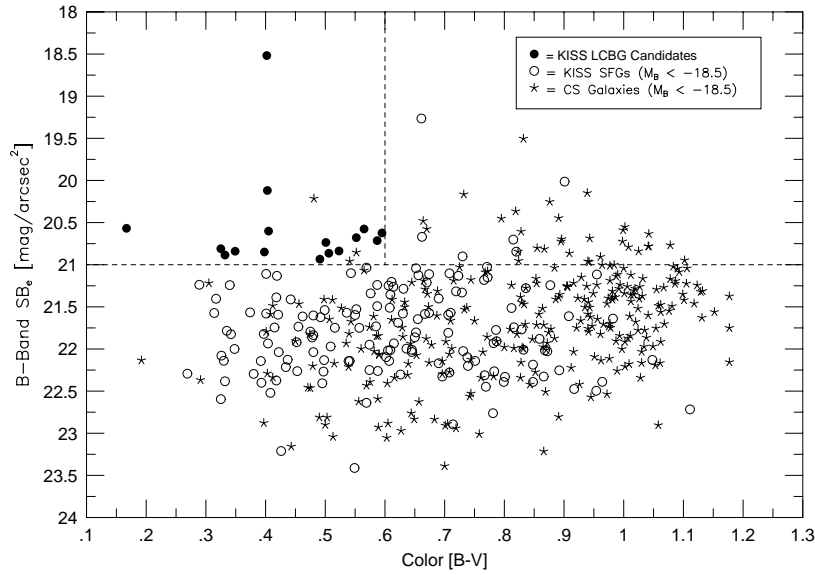


FIG. 4.— Effective  $B$ -band surface brightness plotted against  $B-V$  color for the KISS star-forming galaxies (SFGs) and Century Survey galaxies within 185 Mpc of the Milky Way. Marked by dashed lines are the selection cut-offs for the KISS LCBG sample. A star indicates a galaxy from the CS, and an open circle indicates the KISS SFGs. We see that 16 ELGs comprise the distance-limited LCBG sample, shown by the filled circles.

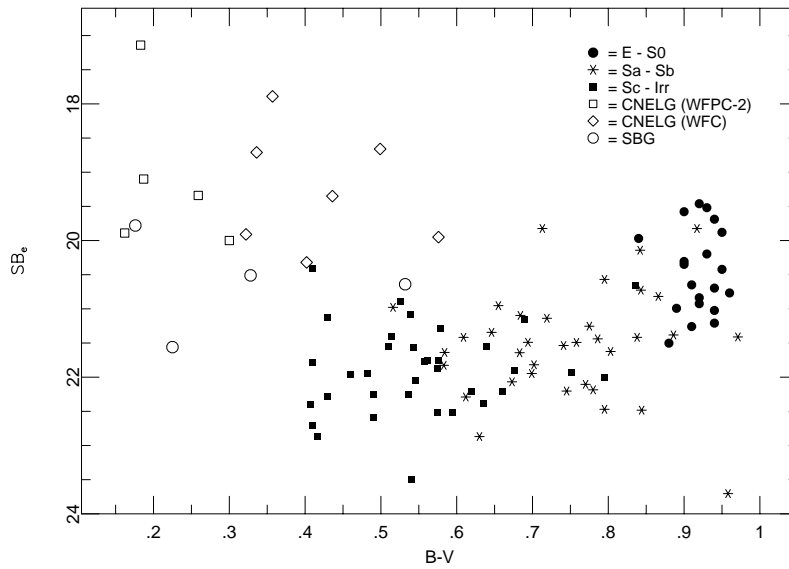


FIG. 5.— Rest-frame effective  $B$ -band surface brightness,  $SB_e$ , versus rest-frame color  $B-V$ . In this plot from Jangren *et al.* (2004), the CNELGs and small, blue galaxies (SBGs), also called faint, blue galaxies, come from Koo *et al.* (1994,1995), while the “normal” Hubble-type galaxies come from a catalog assembled by Frei *et al.* (1996). Here, the LCBGs (CNELGs and SBGs) are clearly separated from the “normal” galaxies. We saw a similar effect in figure 4 for the LCBGs versus the CS galaxies. In contrast, we saw in the same figure that the LCBGs seem to be on the high surface brightness end of a continuous distribution of regular star-forming galaxies.

ity level of a galaxy, telling us how many ionizing stars a galaxy contains. The KISS LCBG candidates have, on average, 60% higher current star-formation rates than the less compact SFGs. There is a clear tendency for the LCBG candidates to be located near the top of the

diagram, again illustrating that they are above average relative to the comparison sample. Note that not all of the LCBG candidates are in the high star-formation rate category. One of the KISS ELGs with the *lowest*  $H\alpha$  luminosity, KISSR 147, happens to be included among the

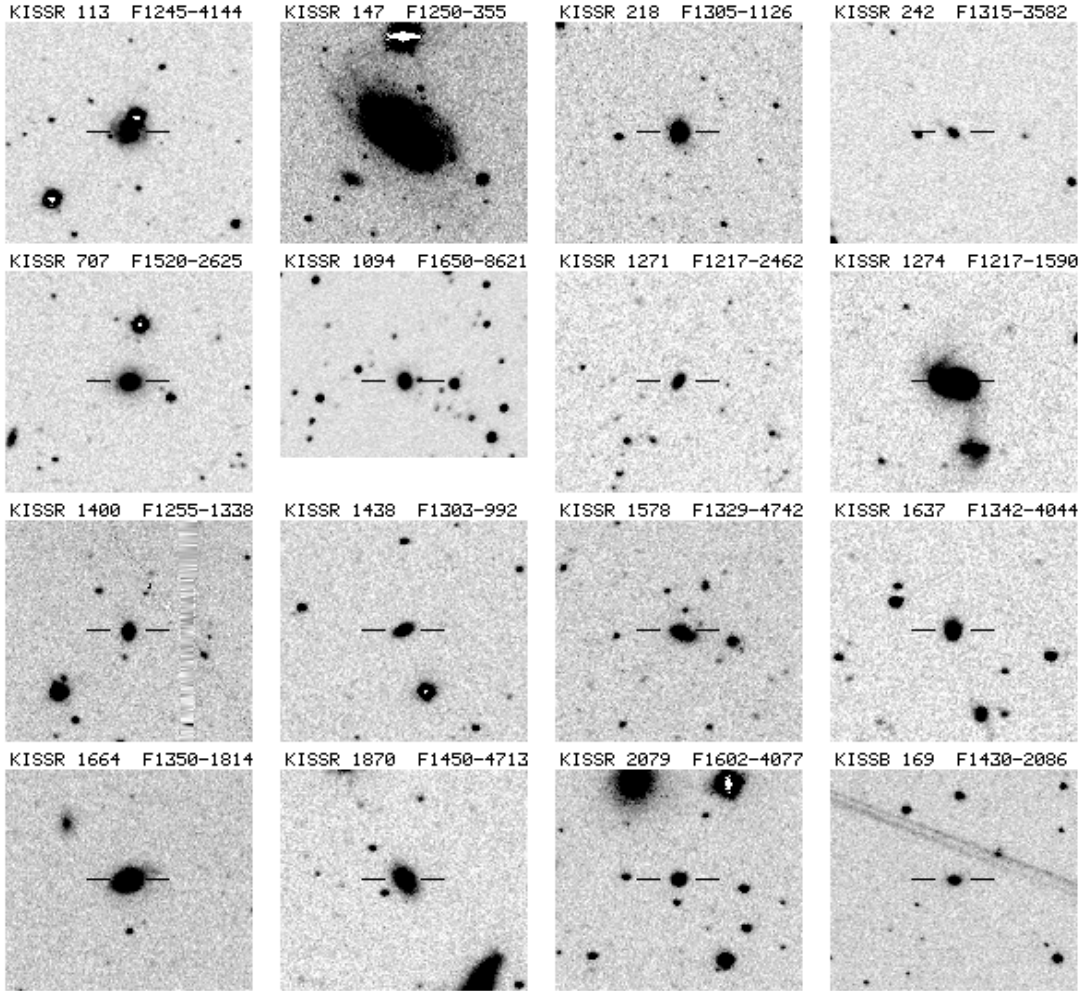


FIG. 6.— Images of all 16 LCBG candidates. These images are derived from the survey images, and represent a composite of the B and V filter direct images. The LCBG candidates are located in the center of each image, and are indicated by the tick marks. For the KR1 and KB1 galaxies (KISSR < 1128, plus KISSB 169) the images cover a FOV of  $4.5 \times 4.0$  arcmin, while those from KR2 (KISSR > 1128) have FOVs of  $3.2 \times 2.9$  arcmin. North is up and East is left in all images.

LCBGs. We note in passing that the measurement of the  $H\alpha$  flux in this object may well be underestimated, since it is so extended on the sky and since the star-formation appears to be spread over a large fraction of the galaxy. The KISS objective-prism flux measurement is made over an 8 arcsec wide region centered on the galaxy. Hence, our current estimate for the  $H\alpha$  luminosity of KISSR 147 may be significantly lower than the actual value. We do not believe that this problem occurs for any of the other KISS LCBGs.

It is also relevant to consider the spectral properties of the LCBG candidates. Do their spectra reveal any systematic differences relative to the less compact SFGs

of the KISS sample? We try to explore this question in two ways. First, in Figure 10, we plot an emission-line ratio diagnostic diagram showing the locations of all of the KISS SFGs (regardless of distance). We plot the logarithms of the  $[O III]/H\beta$  ratio vs. the  $[N II]/H\alpha$  ratio. The smaller open circles are the “regular” star-forming galaxies, while the larger filled symbols indicate the location of the 15 LCBG candidates with measured line ratios. The diagram reveals the characteristic H II sequence, where the SFGs fall along an arc in the diagram stretching from the upper left (typically lower luminosity, lower metallicity galaxies) to the lower right (typically more luminous, higher metallicity objects). The LCBGs

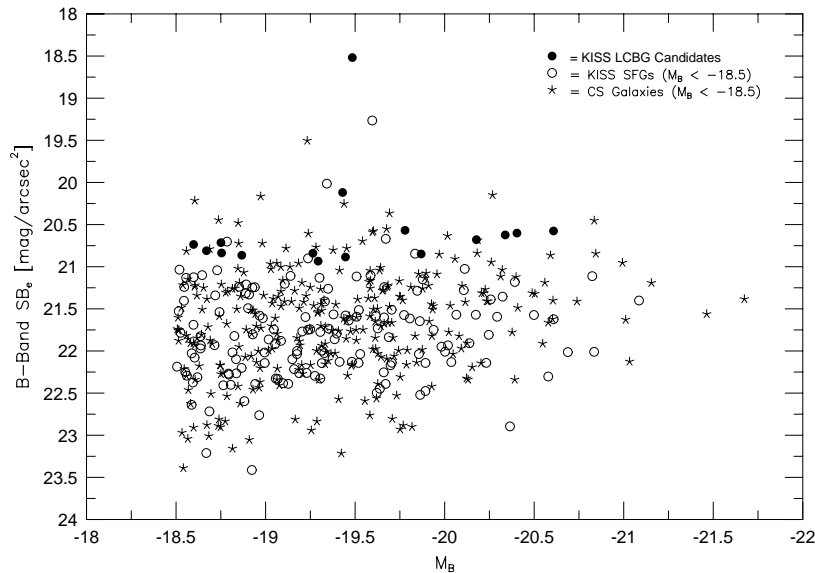


FIG. 7.— The projection of effective  $B$ -band surface brightness against absolute  $B$ -band magnitude for the KISS star-forming galaxies (SFGs) and Century Survey galaxies within 185 Mpc of the Milky Way. A star indicates a galaxy from the CS, and an open circle indicates the KISS SFGs. The distance-limited LCBG sample is shown by the filled circles.

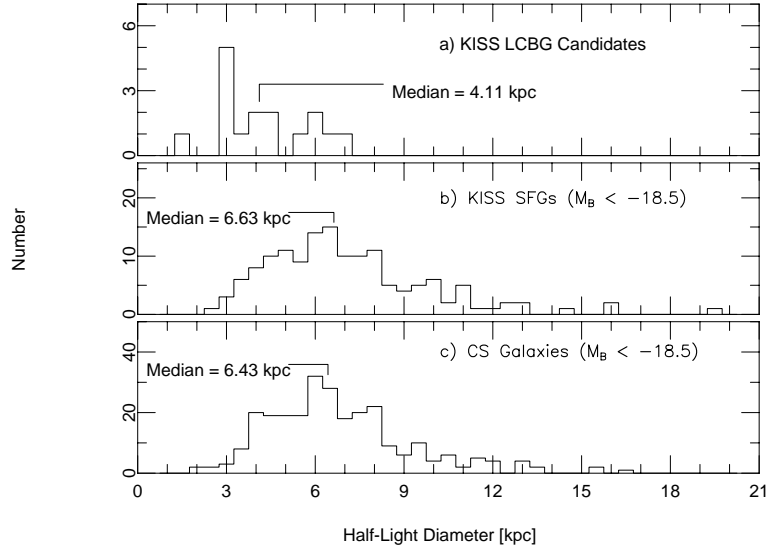


FIG. 8.— Distribution of the derived diameters in kiloparsecs for the 16 KISS LCBG candidates, the comparison sample of KISS SFGs, and the comparison sample of CS galaxies. The median diameter of the LCBG sample is 4.11 kpc, the median diameter of the KISS comparison sample is 6.63 kpc, and the median diameter of the CS comparison sample is 6.43 kpc.

are distributed fairly uniformly along the lower 2/3rds of the arc. Our selection against lower luminosity galaxies prevents them from falling in the upper left portion of the H II sequence. We detect no obvious trends amongst the LCBGs that would lead us to believe that their spectral properties are systematically different from the rest of the KISS SFGs.

We also consider the metal abundances ( $\log(\text{O}/\text{H}) + 12$ ) of these 15 LCBG candidates compared to the sample of all KISS SFGs within 185 Mpc of the Milky Way. Using the linear luminosity-metallicity ( $L-Z$ ) relation of Melbourne & Salzer (2002), we plot metal abundance versus absolute magnitude for the KISS SFGs. Figure 11 shows a weak tendency for the LCBGs, shown as filled

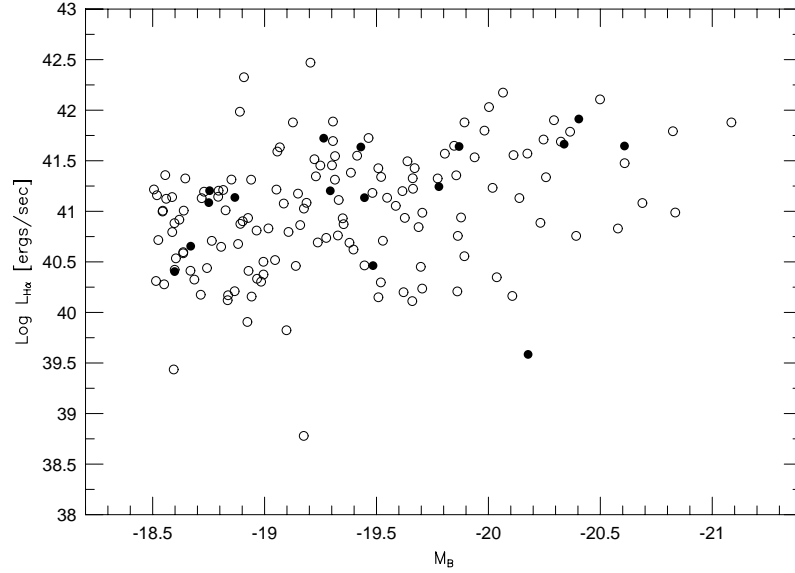


FIG. 9.—  $H\alpha$  luminosities are plotted versus absolute B-band magnitudes for the 16 KISS LCBG candidates (filled circles) and the comparison sample of KISS SFGs (open circles). The median  $\text{Log } L_{H\alpha}$  of this LCBG sample is 41.21 ergs/sec, which is approximately 1.6 times more luminous than the median  $\text{Log } L_{H\alpha}$  of the comparison sample, 41.01 ergs/sec.

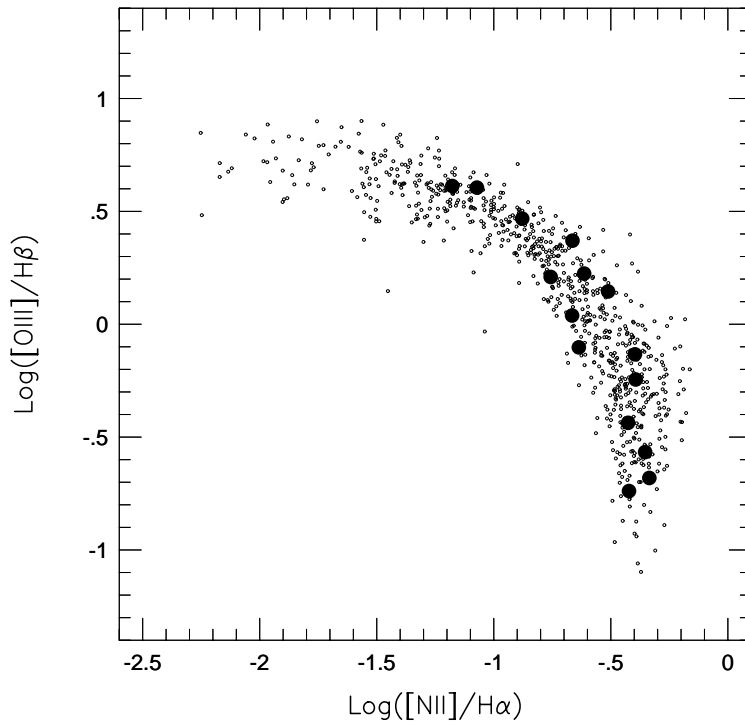


FIG. 10.— A plot of the logarithm of the  $[O\ III]/H\beta$  ratio vs. the logarithm of the  $[N\ II]/H\alpha$  ratio for all KISS SFGs. The large filled circles are the LCBG candidates. The characteristic H II sequence is shown by the KISS SFGs where the low luminosity, metal poor galaxies fall in the upper left of the diagram, and the high luminosity, metal rich galaxies fall in the lower right region. The KISS LCBGs do not appear to deviate from this sequence.

circles on the plot, to lie at or below the mean L-Z relation. The mean abundance of the 15 LCBGs is 8.65, compared to the mean abundance of the comparison sample (KISS SFGs with  $D < 185$  Mpc and  $M_B < -18.5$ ) of 8.75. The statistical significance of this 0.1 dex difference is minimal, since the formal error in the difference of the two means is 0.08. Still, this small difference may suggest that either the LCBGs are under-producing heavy elements compared to the comparison SFGs, are systematically losing a larger fraction of their metals via outflows, or the enhanced star-formation of the LCBGs is producing a modest luminosity enhancement relative to the rest of the SFGs. While it is not possible to definitively select between these options, the high current star-formation rates exhibited by the LCBGs would appear to be inconsistent with the first of these choices, while the higher central mass densities implied by the high  $SB_e$  of the LCBGs is inconsistent with the second (see discussion in Salzer *et al.* (2004)). Hence, we conclude that the LCBG candidates appear to be offset slightly to the left of the KISS SFGs, indicating that their luminosities may not be representative of their masses. While this latter point is likely true in general, for all star-forming galaxies (e.g., Lee *et al.* 2004), it appears to be even more the case for the LCBG sample.

### 3.2. Radio Continuum Emission

To some extent, all galaxies exhibit radio emission, but it is those that are the most radio-luminous that are known historically as “radio-galaxies.” Because star-forming galaxies are often radio sources, we investigate the radio properties of the LCBG candidates as compared to a sample of all KISS SFGs, expecting to detect radio emission for some subset of our samples. All radio fluxes cited in this work come from Van Duyne *et al.* (2004), who used the FIRST (Becker, White & Helfand 1995) and NVSS (Condon *et al.* 1998) 20-cm radio continuum surveys to study the radio emission associated with the 2158 KISS ELGs from KR1 and KR2. Because that study did not include the KB1 portion of KISS, we exclude the KB1 ELGs from this part of our analysis.

13.7% of all KISS ELGs known to be star-forming galaxies in the KR1 and KR2 survey strips are detected by FIRST and NVSS in the radio. This is an upper limit to the fraction of radio-detections, however, since only 57.6% of the KR1 and KR2 galaxies currently have follow-up spectra (note that *all* of the radio-detected KISS galaxies possess follow-up spectra). If we assume that  $\sim 90\%$  of the galaxies lacking follow-up spectra are also SFGs, then the fraction of SFGs with radio continuum detections drops to only 7.4%. This latter value is likely to be closer to the actual percentage of radio-detected SFGs. We compare this number to the fraction of radio galaxies within our LCBG candidate sample (from only KR1 and KR2) and to the fraction of radio galaxies within our distance-limited comparison sample of KR1 and KR2 SFGs with  $M_B < -18.5$ . Fully 53% of the 15 LCBG candidates have detectable radio continuum emission, while 28% of the comparison sample galaxies have detected radio fluxes.

The LCBGs clearly have a stronger propensity to possess detectable radio emission. We hypothesize that the intense star-forming activity indicated by the high  $SB_e$  of the LCBG candidates is the primary contributor to

this effect. In star-forming galaxies, the energy given to the relativistic electrons which cause synchrotron radiation comes from the supernova explosions occurring over the past  $\sim 3 \times 10^7$  years (Cram 1998). Presumably, the KISS LCBGs produce more supernova in this time period than regular star-forming galaxies due to their above-average star formation rates (previous section). Additionally, due to their compact nature, LCBGs may have stronger magnetic fields than regular star-forming galaxies. These properties, in concert, enhance the detectability of synchrotron radiation in LCBGs relative to other star-forming galaxies.

Despite the high proportion of radio detections among the LCBGs, their radio powers do not stand out. For the eight detected LCBGs, the mean radio power is  $10^{21.81} \text{ W Hz}^{-1}$ . This is statistically indistinguishable from the mean of the distance-limited comparison sample ( $10^{21.84} \text{ W Hz}^{-1}$ ), and significantly less than the average of all KISS star-forming galaxies detected by FIRST and NVSS ( $10^{22.11} \text{ W Hz}^{-1}$ ). The majority of the overall radio-detected SFGs lie at distances beyond 185 Mpc, so it is no surprise that their radio luminosities are higher. However, it is perhaps a bit surprising that the LCBGs do not have higher radio powers than the comparison SFGs. Of course, the number of LCBGs in this analysis is small, so it may be premature to draw strong inferences regarding the radio powers at this time. What is clear, however, is that the LCBGs are more commonly detected as radio emitters than are the overall population of star-forming galaxies in the same volume.

### 3.3. Volume Density of Local LCBGs

The space density of the intermediate and high redshift LCBGs compared with that of low redshift LCBGs acts as an essential constraint on their density evolution. Nearly all previous studies of LCBGs stress the apparent extreme density evolution of LCBGs. For our sample of LCBG candidates with  $z < 0.045$  we compute the volume density using the  $1/V_{max}$  method. A complete description of the method along with the specific completeness parameters used in the calculations can be found in Gronwall *et al.* (2004b). In brief, we first determine whether the detectable volume of an individual galaxy is limited by the effective volume set by the KISS redshift limit or by its own emission-line flux. Then, we sum the inverse of the maximum volume within which each galaxy is detectable for all galaxies in this sample. Accordingly, we determine the space density of local LCBGs to be  $5.4 \times 10^{-4} h_{75}^3 \text{ Mpc}^{-3}$ . In order to arrive at an estimate of the uncertainty in the volume density, we will assume that the main source of error is the Poissonian uncertainty in the number of LCBGs (i.e.,  $\sigma = \sqrt{N}$ ). This is reasonable, since the uncertainties in the line flux completeness limits and the relevant volumes are fairly small. Hence, since there are 16 LCBGs in the distance-limited sample, the computed volume density carries with it a 25% uncertainty.

A handful of previous studies have derived estimates for the space densities of LCBGs at intermediate and high redshifts. For example, Phillips *et al.* (1997) find the volume density of LCBGs at redshifts between 0.4 and 0.7 with  $M_B < -18.5$  to be  $2.2 \times 10^{-3} h_{75}^3 \text{ Mpc}^{-3}$ , and that of LCBGs at redshifts between 0.7 and 1.0 with  $M_B < -18.5$  to be  $8.8 \times 10^{-3} h_{75}^3 \text{ Mpc}^{-3}$ . Lowenthal *et al.* (1997)

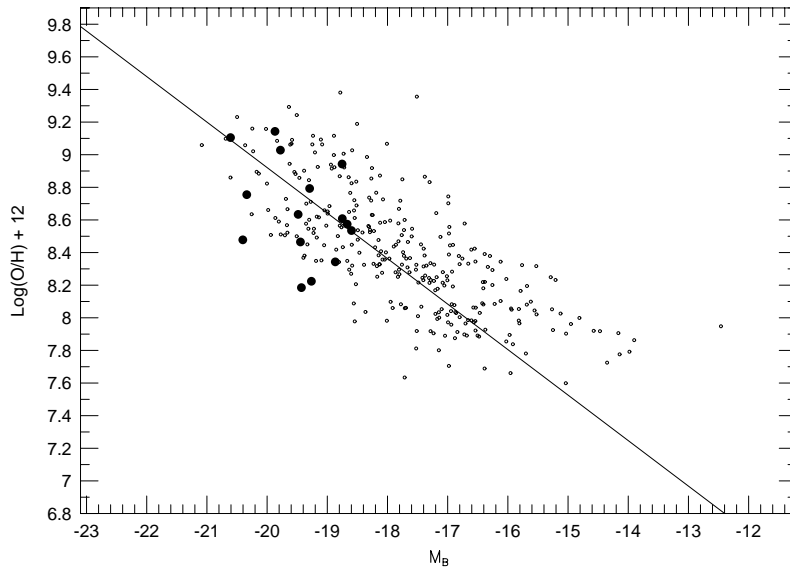


FIG. 11.—  $M_B$  versus the metal abundance ( $\text{Log}(\text{O}/\text{H}) + 12$ ) for KISS SFGs within 185 Mpc of the Milky Way. The 15 LCBG candidates with derived abundances are the filled circles on this plot, and the KISS SFGs are the smaller circles. The line represents the linear L-Z fit for KISS galaxies derived in Melbourne & Salzer (2002).

estimate a total space density of the high redshift ( $2.2 < z < 3.5$ ) population of LCBGs to be  $3.7 \times 10^{-3} h_{75}^3 \text{Mpc}^{-3}$ . This latter density estimate must be taken as a lower limit, since the Lowenthal *et al.* sample is at such high redshifts that only the most luminous sources are detectable. A correction to account for the incompleteness at the lower luminosities would likely raise the density estimate substantially. A large (and probably rather uncertain) incompleteness correction to account for missing lower luminosity LCBGs was applied by Phillips *et al.* to their higher redshift subsample. Because of the large uncertainties associated with the LCBG density estimates in these higher redshift samples, one should use caution in interpreting the numbers. We estimate that the uncertainties in these densities, including any errors associated with the incompleteness corrections, must be at least 33% for the lower redshift value of Phillips *et al.*, and closer to 50% for the two higher redshift estimates.

The uncertainty that arises from different absolute magnitude cut-offs at different redshifts can be alleviated somewhat by applying a **brighter** cut-off to our sample. By making our local sample's luminosity limit consistent with the absolute magnitude limit of the higher- $z$  samples, rather than extrapolating the high- $z$  absolute magnitudes to lower luminosities (as was done by Phillips *et al.* (1997) as described above), one avoids introducing some large and very uncertain corrections. For example, Phillips *et al.* (1997) had an absolute magnitude limit of -20 (using  $H_0 = 50 \text{ km s}^{-1} \text{Mpc}^{-1}$ ) for their sample at  $0.7 < z < 1.0$ , which corresponds to an absolute magnitude limit of -19.12 for  $H_0 = 75 \text{ km s}^{-1} \text{Mpc}^{-1}$ . We derive a volume density of  $3.9 \times 10^{-4} h_{75}^3 \text{Mpc}^{-3}$  for our sample of local LCBGs when we adopt  $M_B = -19.12$  as our luminosity limit. For comparison, Phillips *et al.* (1997) find the volume

density of LCBGs at redshifts between 0.7 and 1.0 with  $M_B < -19.12$  to be  $4.05 \times 10^{-3} h_{75}^3 \text{Mpc}^{-3}$ . We note that this method is impractical to use for the Lowenthal *et al.* sample, and unnecessary when comparing to the lower-redshift Phillips *et al.* sample.

With the above caveats in mind, we compare the volume densities of LCBGs from our local ( $z = 0$ ) sample to those of the higher redshift studies. The value Phillips *et al.* (1997) obtain for their lower redshift sample implies that the volume density of LCBGs has declined by a factor of  $\sim 4$  between  $z \sim 0.5$  and the present, while their higher redshift value suggests that the density of LCBGs has dropped by a factor of  $\sim 16$  between  $z \sim 0.85$  and today. This latter factor becomes  $\sim 10$  for the comparison using the volume density of the KISS LCBGs with  $M_B < -19.12$ . The density drop implied by Lowenthal *et al.* (1997) for the high redshift LCBGs ( $2.2 < z < 3.5$ ) is at least a factor of  $\sim 7$ , and likely to be much higher. The work of Lilly *et al.* (1996); Phillips *et al.* (1997); Lilly *et al.* (1998) and Mallén-Ornelas *et al.* (1999) all suggest that the volume density of LCBGs drops off by a factor of  $\sim 10$  from  $z = 1$  to the present. This prediction is in general agreement with the results presented here, given the large errors associated with the density estimates. That is, the space density derived for our sample of LCBGs compared with that of the higher redshift samples supports the claim that these galaxies are indeed a strongly evolving population. However, the uncertainties associated with the volume density of LCBGs at higher redshifts precludes an accurate assessment of exactly how extreme their evolution is. Hopefully, future studies of high redshift LCBG populations will constrain their volume densities more definitively, and lead to a better understanding of their evolution with look-back time.

## 4. DISCUSSION

This paper deals with the problem of LCBGs by approaching only one of its facets. Namely, we have sought to identify local examples of LCBGs in an effort to constrain the properties of those LCBGs present in such profusion at intermediate- and high- $z$ . However, we must be cautious in accepting that our sample is composed of genuine LCBGs – indeed, we call the galaxies in our sample LCBG candidates. The classification scheme for LCBGs presented by Jangren *et al.* defines a six-dimensional parameter space in which LCBGs are effectively isolated from other types of galaxies. However, we could not apply this method for our LCBG selection, as KISS direct images did not have the resolution required to perform the prescribed tests. And, while Jangren *et al.* conclude that the parameter space of  $B-V$  color vs.  $SB_e$  is the best at separating the LCBGs from other types of galaxies, they acknowledge that there is still no single cut that will eliminate all non-LCBGs nor include all *bona fide* LCBGs.

Specifically, employing a color limit to select local LCBGs based on the corrected rest-frame colors of higher-redshift LCBGs is a bit problematic. The many corrections that must be applied to color, (i.e.,  $K$ -corrections, Galactic reddening, internal extinction, emission-line contamination) make it a difficult parameter to use for defining a sample of galaxies. Additionally, the rest-frame colors of star-forming galaxies at high redshift will be inherently biased to be bluer than those of lower redshift star-forming galaxies. This is because host galaxies at higher redshift have not had as much time to assemble as those in the nearby universe. Hence, they will be intrinsically less luminous, and a star-formation event at high- $z$  will tend to dominate the galaxian color more than at lower redshifts. Accounting for this effect, however, would be a difficult task, mainly because of the uncertainty in our understanding of galaxy evolution.

The necessity of a color parameter, however, is manifest in Figure 4. Luminous elliptical galaxies from the Century Survey meet both the luminosity and surface brightness criteria for LCBGs. However, LCBGs are not similar to local elliptical galaxies. A color cut acts as the means for excluding early-type galaxies in traditional, magnitude-limited surveys. By contrast, in emission-line galaxy surveys such as KISS that contain few, if any, elliptical galaxies, the color criterion becomes less pertinent. Limiting the samples of LCBGs to actively star-forming galaxies should ensure their relative blueness. While not extremely blue compared to other star-forming galaxies, the KISS LCBG candidates are considerably bluer than “normal” galaxies. The Century Survey “normal” field galaxies within the distance limit of 185 Mpc have a median  $B-V$  color of 0.77, considerably higher than the median color of the LCBG sample, 0.44. Were we to have selected a sample of LCBGs using only the luminosity and surface-brightness criteria, and limiting our sample to only actively star-forming galaxies, our sample would have contained 22 KISS LCBG candidates with a median  $B-V$  color of 0.53, still considerably bluer than the CS galaxies.

We select our local samples of LCBGs from only actively star-forming galaxies not only as a way to ensure their relative blueness, but also to further constrain their

properties to match those of the higher-redshift samples. Indeed, all known LCBGs at high- $z$  are vigorously forming stars, as evidenced by their strong emission lines. This property gives rise to important questions regarding the nature of LCBGs. Is active star-formation always present in galaxies meeting the LCBG selection criteria? Can an LCBG be an LCBG without its starburst? What do LCBGs look like when and if the star-formation fades? Do the LCBG criteria allow for non-active galaxies?

In an attempt to address these questions, we looked at the galaxies located in the KISS database that are *not* ELGS, but rather galaxies detected by the Century Survey that have measured redshifts, colors, and absolute magnitudes. Since the first two survey lists of KISS (KR1 and KB1) overlap parts of the CS, we possess direct images taken through  $B$  and  $V$  filters of essentially all of the CS galaxies. By combining our imaging photometry with the CS redshifts (Wegner *et al.* 2001), we are able to carry out the same analysis on the CS galaxies as we previously did for the KISS ELGs. Applying the same cut-offs in  $SB_e$ ,  $M_B$ , and  $B-V$  color to these galaxies yields a sample of seven CS LCBG candidates. Of these, only three were not also detected by KISS. All three lie outside the area of sky covered by KR1. One of these galaxies has been identified using the NASA Extragalactic Database<sup>2</sup> as a nearby Seyfert 2 with very weak emission lines. KISS could not have detected this galaxy due to its strong continuum and the weakness of its  $H\alpha$  line. The others were initially detected by the Case Low-Dispersion Northern Sky Survey (Sanduleak & Pesch 1984), with published follow-up spectroscopy in Salzer *et al.* (1995). One galaxy, CG 60, is a star-forming galaxy with strong  $H\alpha$  and weak  $O III$ . The other, CG 90, appears to be a weak-lined star-forming galaxy, possibly a post-starburst system. This latter galaxy appears to be the closest thing to a “normal” (i.e., not actively star-forming) galaxy in the  $\sim 100$  square degrees of the Century Survey that meets the LCBG selection criteria. However, even CG 90 has *some* current star-formation. The study by Drinkwater *et al.* (1999) which used the Fornax Spectroscopic Survey to find a sample of bright, compact galaxies that are unresolved on photographic plates obtains a similar result. Of their 13 local ( $z < 0.21$ ) galaxies that resemble the higher- $z$  LCBGs, they find only four that do not have strong emission lines. One of the galaxies has a post-starburst spectrum and another has a spectrum indicating an old population.

This paucity of non-active LCBGs suggests that they are, in general, extremely rare, and that perhaps the star-formation that seems always to be present in LCBGs is a key factor to getting labeled as an LCBG in the first place. Clearly the star-formation activity helps to make the LCBG. The starburst will both increase the central luminosity of the galaxy, and lower the half-light radius  $r_{hl}$ . These two effects combine to increase  $SB_e$  and lower the color. Is a central starburst *required* for a galaxy to become an LCBG? Perhaps not, but it certainly appears to be strongly favored.

<sup>2</sup> This research has made use of the NASA/IPAC Extragalactic Database (NED) which is operated by the Jet Propulsion Laboratory, California Institute of Technology, under contract with the National Aeronautics and Space Administration.

While it is possibly premature to attempt to resolve the questions regarding the evolution of LCBGs discussed in §1, we can at least use the properties of the local candidates to speculate a bit. The distribution of the KISS ELGs in Figure 4 suggests that they exhibit a continuum of physical characteristics in the surface brightness, color, and luminosity parameter space. Galaxies classified as LCBGs using the Jangren *et al.* selection criteria represent those galaxies that currently lie at the extreme end of that continuum. Clearly, however, there are plenty of KISS ELGs that are located just below the surface brightness threshold that distinguishes our LCBG candidates from the remainder of the star-forming galaxy population. Since the KISS LCBGs do, on average, exhibit higher H $\alpha$  luminosities, it is likely that at least some of them will evolve out of the LCBG region in Figure 4 as their starbursts fade. Will they fade substantially, as proposed by Koo *et al.* (1995) and Guzmán *et al.* (1998), dropping in luminosity by 4 magnitudes or more, becoming substantially redder and more gas poor and eventually resembling dwarf elliptical galaxies?

We feel that it is unlikely that any of our LCBG candidates will evolve into early-type galaxies. The evolutionary scenario proposed by Koo *et al.* (1995) and Guzmán *et al.* (1998) requires that the gas present in the LCBG be removed, presumably by strong supernovae-driven outflows. Hydrodynamic models (e.g., Mac Low & Ferrara 1999) suggest that this complete blow-away of a galaxy’s ISM does not occur for any but the least massive systems. Therefore, we do not expect any of our current sample of LCBGs to become gas-poor and fade into red ellipticals. Of course, it remains possible that the higher redshift LCBGs represent a more heterogeneous sample of objects (Guzmán *et al.* 1997; Phillips *et al.* 1997; Hammer *et al.* 2001; Pisano *et al.* 2001; Garland *et al.* 2004). If some of the high- $z$  LCBGs did lose their gas and evolve into dwarf elliptical galaxies by the present time, our selection method would not be sensitive to them. However, based on the models of Mac Low & Ferrara, we would expect that the majority of LCBGs should retain their gas to the current epoch. This appears to be the case with our sample.

The continuum of physical characteristics evident in Figure 4 suggests that luminous galaxies possess a range in their central surface brightnesses / central mass densities. This has previously been observed in dwarf galaxies (e.g., Papaderos *et al.* 1996, Salzer & Norton 1999), where the most actively star-forming dwarf galaxies (a.k.a. blue compact dwarfs, or BCDs) are seen to lie at the extreme end of a continuum that stretches to very low central surface brightnesses at the other extreme. Furthermore, the gas distributions in the BCDs are seen to be much more centrally concentrated than those in more quiescent dwarf irregulars (e.g., van Zee, Skillman & Salzer 1998). The combination of high central mass densities and high central gas densities make BCDs particularly efficient at forming stars. We assume that this is no accident: BCDs are by their nature well equipped to be making stars. By analogy, one might argue that LCBGs are predisposed to make stars efficiently because they too represent the extreme high surface brightness, high central mass density end of a continuous distribution, albeit for more luminous galaxies. In this picture, LCBGs are preferentially in a star-forming phase for a large fraction of the time.

When not undergoing a strong starburst, they will fade somewhat (mostly in SB $_e$ , but also slightly in color and luminosity) and join the population of galaxies lying below the LCBG selection region in Figure 4. This would help to explain the lack of *any* non-star-forming LCBGs present among the CS galaxies. Even when not strongly bursting, post LCBGs may exhibit a modest level of star formation, such as that seen in CG 90. The question of where the large population of LCBGs seen at  $z = 0.5$  to 1.0 has gone is then resolved, at least in part, by the population of less actively star-forming galaxies seen in Figure 4. The large number of KISS ELGs located below the LCBG selection region in this plot appear to be able to account for a large fraction of the “missing” LCBGs. The drop in density of LCBGs may be directly linked to the fall in the star-formation rate density between  $z = 1$  to the present (e.g., Madau *et al.* 1996, 1998). The galaxies still exist, they are simply in a somewhat less active state. In this scenario, LCBGs are not pathological outliers, but rather the most compact galaxies at the extreme end of a continuous distribution of gas-rich star-forming galaxies.

It should be relatively simple to test the above hypothesis. A combination of high spatial resolution surface photometry in the optical and VLA HI mapping in the radio could be used to evaluate the stellar- and gas-mass distributions of the local LCBG candidates. A direct comparison of these properties between the LCBGs and a sample of “normal” galaxies would reveal whether our LCBGs are structurally different from the non-LCBGs. These same observations would be extremely helpful in establishing their dynamical masses as well. This latter parameter is essential for showing clearer linkage between the local samples of LCBGs with the intermediate- and high-redshift analogues. Efforts are already underway in this regard. As a first step in determining gas and dynamical masses, we have obtained single-dish HI observations with the Arecibo 305-m radio telescope for the sample of LCBGs accessible from Arecibo, along with a control sample of “normal” star-forming galaxies. With these data, we will derive HI masses and provide at least a rough estimate for the dynamical masses (Werk *et al.* 2005) for our LCBGs. We will also be able to ascertain which of our galaxies would be suitable for follow-up VLA mapping. In addition, we have begun acquiring higher resolution optical images of our LCBGs, with the goal of being able to perform detailed surface photometry. In addition, these more detailed images will allow us to carry out a morphological analysis of our sample of local LCBGs, that will provide clues as to whether their intense starbursts are caused by mergers and/or interactions, or are simply the result of their intrinsically compact nature. Finally emission line-widths measured from high-resolution spectra combined with near-infrared images and our HI mass estimates could settle the debate about the masses of LCBGs.

## 5. SUMMARY AND CONCLUSIONS

In this paper, we present a sample of local analogues to the intermediate- and high- $z$  LCBGs. We selected our sample from only those KISS galaxies that are actively forming stars. Due to resolution effects, we limit our sample to only those galaxies within 185 Mpc of the Milky Way. The sample of LCBGs is defined by the fol-

lowing criteria: a surface brightness limit of  $SB_e < 21.0$  mag arcsec $^{-2}$ , an absolute magnitude limit of  $M_B < -18.5$ , and a color cut-off of  $B - V < 0.6$  with  $H_0 = 75$  km s $^{-1}$  Mpc $^{-1}$ . A total of 16 KISS SFGs meet these criteria.

We have compared some of the properties of the KISS LCBG candidates to those of a comparison sample of KISS SFGs, and a comparison sample of Century Survey (CS) galaxies that are supposed to represent “normal galaxies.” On average, the KISS LCBG candidates have a higher tendency to emit detectable radio continuum flux, have higher H $\alpha$  luminosities indicating strong star-formation properties, have slightly lower than expected metal abundances for KISS galaxies of their luminosity, and considerably smaller size than those galaxies in both KISS and CS comparison samples. We have calculated the volume density for the sample of local LCBG candidates to be  $5.4 \times 10^{-4} h_{75}^3 \text{Mpc}^{-3}$ . This value indicates a substantial density evolution of LCBGs, which is in general agreement with the predictions made by Lilly *et al.* (1996); Phillips *et al.* (1997); Lilly *et al.* (1998) and Mallén-Ornelas *et al.* (1999). However, precise estimates of the density evolution of the LCBGs are difficult, due to the large uncertainties in the values of the volume density for higher-redshift populations. We have utilized the CS database in an attempt to select a sample of local non-active LCBGs in order to constrain the density of non-star-forming LCBGs. We found no additional non-star-forming LCBGs, although one weakly star-forming (possibly post-starburst) galaxy was recognized. We postulate that LCBGs are structurally predisposed for star-formation, and that their compact nature may be indicative of a high central gas concentration that

drives ongoing star-formation.

The need for a local sample of LCBGs is well documented. Much of the published work on these galaxies speaks to the need for a representative local comparison sample that will help settle the debates over their size and mass, morphology, and low-redshift counterparts. We conclude that our sample of local LCBG candidates contains galaxies that are likely to be local versions of the more distant LCBGs. This local sample provides the starting point in our ongoing study of the properties and evolution of LCBGs.

Funding for this work was provided by an NSF Presidential Faculty Award to JJS (NSF-AST-9553020). Additional support for our ongoing follow-up spectroscopy campaign came from continued funding from the NSF (NSF-AST-0071114) and Wesleyan University. We are grateful to the anonymous referee for several helpful suggestions that improved the presentation. We thank the numerous KISS team members who have participated in spectroscopic follow-up observations during the past several years, particularly Caryl Gronwall, Drew Phillips, Gary Wegner, Jason Melbourne, Laura Chomiuk, Kerrie McKinstry, Robin Ciardullo, and Vicki Sarajedini. Special thanks to Rafael Guzmán for providing us with information about selection criteria for LCBGs, and several useful discussions. Finally, we wish to thank the support staffs of Kitt Peak National Observatory, Lick Observatory, the Hobby-Eberly Telescope, MDM Observatory, and Apache Point Observatory for their excellent assistance in obtaining both the survey data as well as the spectroscopic observations.

#### REFERENCES

- Barton, E. J., & van Zee, L. 2001, ApJ, 550, L35  
 Becker, R. H., White, R. L., & Helfand, D. J. 1995, ApJ, 450, 559  
 Castander, F. J., *et al.* 2004, in preparation  
 Condon, J. J., Cotton, W. D., Griesen, E. W., Yin, Q. F., Perley, R. A., Taylor, G. B., & Broderick, J. J. 1998, AJ, 115, 1693  
 Cram, L. E. 1998, ApJ, 506, L85  
 Drinkwater, M. J., Phillips, S., Gregg, M. D., Parker, Q. A., Smith, R. M., Davies, J. I., Jones, J. B., & Sadler, E. M. 1999, ApJ, 511, L97  
 Frei, Z., Guhathakurta, P., Gunn, J. E., & Tyson, J. A. 1996, AJ, 111, 174  
 Garland, C. A., Pisano, D. J., Williams, J. P., Guzmán, R., Castander, F. J. 2004, ApJ, in press  
 Geller, M. J., Kurtz, M. J., Wegner, G., Thorstensen, J. R., Fabricant, D. G., Marzke, R. O., Huchra, J. P., Schild, R. E., & Falco, E. E. 1997, AJ, 114, 2205  
 Gronwall, C., Jangren A., Salzer, J. J., Werk, J. K., & Ciardullo, R. 2004a, AJ, 128, 644  
 Gronwall, C., Salzer, J. J., Brenneman, L., Condy, E., & Santos, M. 2004b, AJ, in preparation  
 Gronwall, C., Salzer, J. J., Sarajedini, V. L., Jangren, A., Chomiuk, L., Moody, J. W., Frattare, L. M., & Boroson, T. A. 2004c, AJ, 127, 1943 (KR2)  
 Guzmán, R. 2001, Ap&SS, 277, 507  
 Guzmán, R., 2003, in *Proceedings of the ESO/USM/MPE Workshop on Multiwavelength Mapping of Galaxy Formation and Evolution*, Eds. Bender R., & Renzini A., Springer-Verlag  
 Guzmán, R., Gallego, J., Koo, D. C., Phillips, A. C., Lowenthal, J. D., Faber, S. M., Illingworth, G. D., Vogt, N. P. 1997, ApJ, 489, 559  
 Guzmán, R., Jangren, A., Koo, D. C., Bershady, M. A., Simard, L. 1998, ApJ, 495, L13  
 Guzmán, R., Koo, D. C., Faber, M., Illingworth, G., Takamiya, M., Kron, R. G., & Bershady, M. A. 1996, ApJ, 460, L5  
 Guzmán, R., Östlin, G., Kunth, D., Bershady, M. A., Koo, D. C., & Pahre, M. A. 2003, ApJ, 586, L45  
 Hammer, F., Gruel, N., Thuan, T. X., Flores, H., Infante, L. 2001, ApJ, 550, 570  
 Jangren, A., Bershady, M. A., Conselice, C. J., Koo, D. C., Guzmán, R. 2004, in preparation  
 Koo, D. C., Bershady, M. A., Wirth, G. D., Stanford, S. A., & Majewski, S. R. 1994, ApJ, 427, L9  
 Koo, D. C., Guzmán, R., Faber, S. M., Illingworth, G. D., Bershady, M. A., Kron, R. G., & Takamiya, M. 1995, ApJ, 440, L49  
 Koo, D. C., Kron, R. G. 1992, ARA&A, 30 613  
 Lee, J. C., Salzer, J. J., & Melbourne, J. 2004, ApJ, in press  
 Lilly, S., Le Fèvre, O., Hammer, F., & Crampton, D. 1996, ApJ, 460, L1  
 Lilly, S. J. *et al.* 1998, ApJ, 500, 75  
 Lowenthal, J. D., Koo, D. C., Guzmán, R., Faber, S. M., Vogt, N. P., Illingworth, G. D., & Gronwall, C. 1997, ApJ, 489, 673  
 Mac Low, M., & Ferrara, A. 1999, ApJ, 513, 142  
 Madau, P., Ferguson, H. C., Dickinson, M. E., Giavalisco, M., Steidel, C. C., & Fruchter, A. 1996, MNRAS, 283, 1388  
 Madau, P., Pozzetti, L., & Dickinson, M. E. 1998, ApJ, 498, 106  
 Mallén-Ornelas, G., Lilly, S. J., Crampton, D., Schade, D. 1999, ApJ, 518, L83  
 Melbourne, J., Phillips, A. C., Salzer, J. J., Gronwall, C., & Sarajedini, V. L. 2004, AJ, 127, 686  
 Melbourne, J., & Salzer, J. J. 2002, AJ, 123, 2302  
 Östlin, G., Amram, P., Bergvall, N., Masegosa, J., Boulesteix, J., Márquez, I. 2001a, *ã*, 374, 800  
 Östlin, G., Amram, P., Boulesteix, J., Bergvall, N., Masegosa, J., Márquez, I. 2001b, Ap&SS, 277, 433  
 Papaderos, P., Loose, H. H., Fricke, K. J., & Thuan, T. X. 1996, A&A, 314, 59

- Phillips, A. C., Guzmán, R., Gallego, J., Koo, D. C., Lowenthal, J. D., Vogt, N. P., Faber, S. M., Illingworth, G. D. 1997, ApJ, 489, 543
- Pisano, D. J., Kobulnicky, H. A., Guzmán, R., Gallego, J., Bershad, M. A. 2001, AJ, 122, 1194
- Salzer, J. J., Gronwall, C., Lipovetsky, V. A., Kniazev, A., Moody, J. W., Boroson, T. A., Thuan, T. X., Izotov, Y. I., Herrero, J. L., Frattare, L. M. 2000, AJ, 120, 80
- Salzer, J. J., Gronwall, C., Lipovetsky, V. A., Kniazev, A., Moody, J. W., Boroson, T. A., Thuan, T. X., Izotov, Y. I., Herrero, J. L., Frattare, L. M. 2001, AJ, 121, 66
- Salzer, J. J., Gronwall, C., Sarajedini, V.L., Lipovetsky, V. A., Kniazev, A., Moody, J. W., Boroson, T. A., Thuan, T. X., Izotov, Y. I., Herrero, J. L., Frattare, L. M. 2001, AJ, 123, 1292
- Salzer, J. J., Lee, J. C., Melbourne, J., Hinz, J., Alonso-Herrero, A., & Jangren, A. 2004, in preparation
- Salzer, J. J., Moody, J. W., Rosenberg, J., Gregory, S. A., & Newberry, M.V. 1995, AJ, 109, 2376
- Salzer, J. J., & Norton, S. A. 1999, in *The Low Surface Brightness Universe*, ASP Conference Series 170. Ed: J.I. Davies, C. Impey, and S. Phillipps pg 253
- Sanduleak, N., Pesch, P. 1984 ApJS, 55, 517
- Schade, D., Lilly, S. J., Crampton, D., Hammer, F., Le Fèvre, O., & Tresse, L. 1995, ApJ, 451, L1
- Schade, D., Lilly, S. J., Le Fèvre, O., Hammer, F., & Crampton, D. 1996, ApJ, 464, 79
- Schlegel, D. J., Finkbeiner, D. P., & Davis, M. 1998, ApJ, 500, 525
- Smail, I., Ivison, R. J., Blain, A. W., & Kneib, J. P. 1998, ApJ, 507, L21
- Van Duyne, J., Beckerman, E., Salzer, J. J., Gronwall, C., Thuan, T. X., Condon, J. J., & Frattare, L. M. 2004, AJ, 127, 1959
- van Zee, L., Skillman, E. D., & Salzer, J. J. 1998, AJ, 116, 1186
- Wegner, G., *et al.* 2001, AJ, 122, 2893
- Wegner, G., Salzer, J. J., Gronwall, C., Jangren, A., & Melbourne, J. 2003 AJ, 125, 2373
- Werk, J. K., Salzer, J. J., Jangren, A., Melbourne, J., & Lee, J. C. 2005, in preparation

TABLE 1  
A KISS SAMPLE OF LCBG CANDIDATES.

KISSR # (1)	KISSB # (2)	$m_B$ (3)	B-V (4)	Diameter kpc (5)	$SB_e$ mag/arcsec <sup>2</sup> (6)	Dist Mpc (7)	$M_B$ (8)	$\log L_{H\alpha}$ ergs/s (9)	$\log P_{1.4GHz}$ Watts/Hz (10)
113	...	15.36	0.40	1.53	18.52	93	-19.48	40.46	...
147	...	12.44	0.55	6.53	20.68	33	-20.18	39.59	22.19
218	...	15.34	0.49	4.21	20.93	84	-19.29	41.20	21.60
242	128	16.66	0.35	4.02	20.84	153	-19.26	41.72	21.62
...	169	16.56	0.51	3.39	20.86	122	-18.87	41.14	...
707	189	14.99	0.40	5.42	20.85	94	-19.87	41.64	21.41
1094	218	15.24	0.41	6.08	20.60	134	-20.40	41.91	21.86
1271	...	17.33	0.50	2.82	20.74	153	-18.60	40.40	...
1274	...	14.37	0.57	6.91	20.58	99	-20.61	41.65	21.89
1400	...	16.45	0.17	4.49	20.57	176	-19.78	41.24	...
1438	...	16.52	0.33	3.01	20.81	109	-18.67	40.66	...
1578	...	15.85	0.40	3.11	20.12	114	-19.43	41.64	21.71
1637	...	16.30	0.33	4.46	20.89	141	-19.44	41.14	...
1664	...	15.33	0.60	5.96	20.62	136	-20.34	41.66	22.22
1870	...	15.66	0.59	2.99	20.71	76	-18.75	41.09	...
2079	...	16.80	0.52	3.17	20.84	129	-18.75	41.20	...